Egypt. J. Chem. **Vol. 67,** No. 4 pp. 165 - 179 (2024)

Egyptian Journal of Chemistry

http://ejchem.journals.ekb.eg/

Bio-Remediation of Cationic Dyes Using Composite Polymer Sheets of Cellulose Acetate and Unhydrolyzed Sugarcane Bagasse Wastes

H. M. Magdy[1], Hekmat R. Madian[1], Ahmed E. Abdelhamid[2*], M.M. Hegazi[3], A. Labena[1]

[1]*Egyptian Petroleum Research Institute (EPRI), Nasr City, Cairo, 11727, Egypt.*

[2] *Polymers & Pigments Department, National Research Centre (NRC), Dokki, Cairo, 12622, Egypt.*

[3]Faculty of Agriculture, Ain Shams University, Cairo, Egypt.

Abstract

This study was directed to use the sugarcane bagasse wastes as bio-sorbent materials to remove cationic dyes; Methylene Blue (MB) and Crystal Violet (CV), from synthetic industrial wastewater. The collected and dried sugarcane bagasse wastes were treated with different concentration of H_2SO_4 as a pre-treatment step in the production of bioethanol after hydrolyzing the lignin content. Afterwards, the unhydrolyzed wastes were dried and ground with a ball mill then mixed with cellulose acetate to form composite sheets that directed to biosorption process. The composite sheets were functionally and structurally explored using FT-IR, XRD, SEM, swelling and the porosity. Optimization of the biosorption processes were performed using "One Factor at A Time (OFAT)" and subsequently "a full factorial design". Results displayed that, the MB removal efficiency of 90.36% was accomplished using a composite sheet dose of 5 g/l treated with 4% H_2SO_4 for 100 ppm MB after 240 min. In addition, the CV removal efficiency of 89.29 % was obtained by using the same composite sheet with dose of 7g/l for removing of 500 ppm CV after 240 min. Isotherms and Kinetics models were also examined. Moreover, the reusability experiment was demonstrated for 5-times use. In conclusion, the unhydrolyzed sugarcane bagasse wastes, that remained after treated with different sulfuric acid concentrations, combined with cellulose acetate were successfully provide different composite sheets that applied in the 3Rs processes, Removal, Recover and Reuse of the MB and CV dyes.

Keywords: Agriculture Wastes; Sugarcane Bagasse; Industrial Wastewater; Adsorption; Polymer Composite; Methylene Blue; Crystal Violet

1. Introduction

Nowadays Egypt is facing countless of problems that attributed to water availability and scarcity **[1, 2]**. The Minister of Resources and Irrigation has stated many barriers that face the Egyptian unstable climate, limited Nile water amount and the huge increasing in population growth **[3].** Industrial discharges, which contain a variety of toxic and hazardous chemicals such as heavy metals, dyes and other organic and inorganic materials, are the main source of water pollution that may contaminate the available water resources. Industrial wastewater is considered as the most significant causes of pollution, that harming human being **[4-6].** Dyes, for example, have a long-term durability, low solubility, fast binding action and induce problems, even at a lower concentration **[7]**. Cationic dyes for example; Methylene Blue (MB) & Crystal Violet (CV) are types of toxic chemicals that are used as a coloring agent for textile, and paints industry. These dyes have a harmful effect on environment, ecosystems, and human health **[8-9]**. Different physicochemical conventional techniques were investigated to help such industries to eliminate the MB and CV dyes from their effluents before discharging. Moreover, these techniques had a lot of disadvantages such as their high-cost, and generation of hazardous wastes after the treatment process **[10]**. In addition, there are many desired techniques including adsorption, nano filtration, ozonation, and electro flotation that may use in this matter **[11].**

*Corresponding author e-mail: ahmednrc10@gmail.com.; (Ahmed E Abdelhamid).

Receive Date: 16 August 2023, **Revise Date:** 25 September 2023, **Accept Date:** 10 October 2023

DOI: 10.21608/EJCHEM.2023.229672.8443

Among them, adsorption, using agriculture biomasses such as sugarcane bagasse wastes, is still the best choice for the contaminated wastewater treatment **[12]**. The sugarcane bagasse wastes are considered one of the largest biomass in Egypt and worldwide **[13]**. They have been previously reported to be used as a feedstock in the production of bioethanol and other applications **[14, 15].** To produce the bioethanol from the sugarcane bagasse wastes, it should pre-treat first to degrade the lignin content and liberate the available cellulose and hemicellulos **[16, 17]**. After the pre-treatment method and the bioethanol production, the residual unhydrolyzed wastes afterwards provide highly charged materials that can be used as excellent sorbents. However, application of the sugarcane bagasse wastes, in their usable form, provides a low surface area which reflected in their removal efficiency performance reduction and prevent the replicability option. Incorporation of adsorbent materials in porous polymer matrix can enhance the adsorption capacity and can be produced in different forms as beads or sheet **[18, 19]**. Therefore, this study was directed to grind the unhydrolyzed sugarcane bagasse wastes, residual wastes after pre-treatment and be used in the production of bioethanol, with a ball milling method to increase their surface area and an easily mix with cellulose acetate forming different composite sheets. The pre-treatment process was displayed in four systems as (1) 20g bagasse with 2% H_2SO_4, (2)20g bagasse with 4% H_2SO_4, (3) 10g bagasse with 4% H_2SO_4, and (4) 10g bagasse with 2% H_2SO_4 in addition to the blank composite sheet (cellulose acetate without any unhydrolyzed bagasse wastes) and the control composite sheet (cellulose acetate with the bagasse substrate without any pre-treatment).

The aim of the present work is to prepare, characterize, and evaluate polymer composite sheets from cellulose acetate and sugarcane bagasse waste for removal of cationic dyes as methylene blue and crystal violet. The composite sheets were characterized by different techniques to determine their structure, functionality and reactivity using i.e.; Fourier transform infrared (FT-IR), (X-ray) diffraction (XRD), Scanning electron microscopy (SEM), Swelling, Porosity and Zeta potentials. Optimizing the adsorption processes using "One Factor at A Time (OAFT) and full factorial design" were performed. Furthermore, isotherms and kinetics models were studied to predict the mode of adsorption for each dye. Afterwards, the 3Rs (removal, recover, reuse) processes were obtained via reusability experiments for the highest removal efficiency composite sheets as an example for the all sheets **[20, 21]**.

2. Materials and methods

2.1. Sorbent preparation and composite sheet formation

The sugarcane bagasse wastes were obtained from the Egyptian`s market, dried for a week, cut by a scissor, ground by a mixer, and sieved to relatively have a size of 0.5–1 cm. The materials were afterwards stored at a room temperature until analyses and pre-treatment process. The pre-treatment process includes two concentrations of the sugarcane bagasse (10 and 20 g), two concentrations of H_2SO_4 (2% and 4% v/v) that mixed separately in an Erlenmeyer flask (250 ml). Each flask was closed and autoclaved for 20 min at 121 °C. Afterwards, the flasks were filtered after hydrolysis to remove the unhydrolyzed wastes. Then, the filtrates were neutralized, centrifuged for 10 min at 10,000 rpm. The filtrates were used for the bioethanol production (Data not shown). The unhydrolyzed materials were distinguished as; (1) 20g sugarcane bagasse waste treated with 2% H_2SO_4, (2) 20g sugarcane bagasse waste treated with 4% H_2SO_4, (3) 10g sugarcane bagasse waste treated with 4% H_2SO_4, and (4) 10g sugarcane bagasse waste treated with 2% H_2SO_4. In addition, sugarcane bagasse waste without any pre-treatment was used as a control material. Afterwards, cellulose, hemicellulose and lignin percent of all materials were measured in "the Agricultural Research Center, Giza, Egypt". In order to increase the surface area of the bio-sorbent material (unhydrolyzed sugarcane bagasse wastes), it was ground to the smallest size using a ball mailing "Planetary Ball Mill PM 400, grinding stations Malvern UK". The ground materials particle-size and zeta potentials were estimated by Dynamic Light Scattering (DLS) [Nano-25, Malvern UK]. The particle size of the samples were explored as follow; 286.8, 455, 116, 291.4 and 295.8 nm for the materials of 1, 2, 3, 4, control, respectively. Afterwards, a 1.8 gm of cellulose acetate was mixed with 10 ml of Dimethylformamide (DMF) solvent. Then different doses of the unhydrolyzed bagasse wastes (1,2,3, and 4) in addition to a blank (cellulose acetate without any unhydrolyzed sugarcane bagasse wastes) and a control (cellulose acetate with the sugarcane bagasse substrate

without any pre-treatment), were added separately to the solution, stirred, and left to form a homogenous mixture. After that, the mixtures were casted onto a clean and dry glass plate that is tightly settled with a masking tape. By using a film applicator, the mixtures were spread out wisely without forming any bubbles in order to form a good sheet **[22]**.the casted films were immersed directly into the coagulation water bath and left for 24 h with changing the water twice in order to remove the residual solvent from the precipitated sheets. The sheets were removed and air dried to be ready for characterization and application.

2.2. Characterization of the polymer sheets

2.2.1. Fourier transform infrared (FT-IR)

The FT-IR spectroscopy was applied in this study to estimate the change in vibration frequency of the composite sheets. The spectra were gathered using "Nicolet IS-10 spectroscopy, German" with a wavelength range of 400 – 4000 cm^{-1}.

2.2.2. X-ray diffraction (XRD)

The XRD patterns were detected by the X'Pert PRO PAN analytical apparatus, which is a commonly used instrument for analyzing crystal structures. The XRD measurements were conducted using CuKa radiation, which has a wavelength of 0.1541 nanometers. The data was collected within the 2θ range from 10° to 90°. The step size used was 0.02°, which means that the instrument recorded the diffraction pattern of the composite sheets at small intervals within the specified 2θ range.

2.2.3. Scanning electron microscopy (SEM)

The morphology of the composite sheets was assessed using scanning electron microscopy (SEM). This technique was operated with an accelerating voltage of 15 kV "(Hitachi SE 900)" and a magnification of 5000×.

2.2.4. Swelling

The swelling behaviors of the composite sheets were determined by immersing 5×5 cm^2 from the composite sheets (1, 2, 3, and 4) in water for one day. The composite sheet's wet weights were achieved after wiping the excess distilled water by a tissue. Afterwards, the composite sheets were dried till have a constant weight at 100ºC, as previously reported **[23]**.

2.2.5. Porosity

The porosity attitudes of the composite sheets were evaluated according to their wet and dry weight method, as previously reported **[24].**

2.3. Application of the composite sheets in the removal of Methylene Blue (MB) and Crystal Violet (CV) from contaminated wastewater

2.3.1. Adsorbate preparation

Stoke solutions of the used dyes (MB and CV) at a concentration of 1000 ppm were prepared by dissolving anaccurately weighed amount of the individual dye in water. Subsequently, from this stoke solution, desired concentrations of absorbents 50, 100, and 150 ppm were prepared. The maximum absorbance (λ_{max}) of the dyes was determined using UV-vis spectrophotometer "Cary 100, Agilent Technologies, Santa Clara, CA, USA" at different wavelengths with a correlation to the used dyes i.e., at 664 nm for the MB and 590 nm for the CV**.**

2.3.2. Screening experiment

One g/l from each composite sheet was placed in the dye solution and shaken for 3h at 100 rpm. At the end of the experiment, the concentrations of dyes before and after the experiment were checked by the spectroscopy at wavelengths of 664 nm for the MB and 590 nm for the CV. Finally, the removal efficiencies (RE) were estimated according to next equation.

$$Removal\ effeciency\ (\%) = \frac{C_o - C_e}{C_o} \times 100$$

Where C_o is the initial concentration, C_e is the final concentration of the used dyes.

2.4. Optimization processes

The removal efficiencies of the dyes, using the selected composite sheets after screening experiment, were optimized via two steps, OFAT, to estimate the high and low levels of each factor, then "full factorial design experiments".

2.4.1. One factor at A Time (OFAT) experiments

Different contact time were investigated; 30, 60, 90, 120, 180 and 240 min. Then different pH values were tested; 3, 5, 7, and 9. Afterwards, different dosages of the composite sheets were investigated; 2, 5, 7 g/l. Moreover, the change in the MB and the CV dye`s concentrations; 100, 200, 300, and 500 ppm were also estimated in the OFAT experiments, change one factor and fix the others.

2.4.2. General Full factorial design experiments

General full factorial design experiments ($2^{3*}3^{1}$) were run for the selected composite sheets in order to summarize the best factors that give the highest removal efficiencies for each dye. The levels of the factors were reported in **Table S1** for the MB and the CV used dyes. The Factorial design matrix and the achieved dyes removal efficiencies, with fits and residuals values, were reported. The effect of the experimental variables was attempted; contact time intervals, pH values, composite dose and dye concentration. The results were assumed by the Minitab 18 software.

2.5. Langmuir and Freundlich isotherms

For the aim of the MB and CV adsorption mechanism determination by using the selected composite sheets, as adsorbent materials, the linear Langmuir and Freundlich isotherms were checked as previously reported **[25, 26].** The equations expressed to the Langmuir isotherm and the Freundlich isotherm are illustrated as follows

Langmuir isotherm model equation:

$$\frac{Ce}{qe} = \frac{Ce}{qmax} + \frac{1}{bqmax}$$

Freundlich isotherm model equation:

$$Ln\ qe = LnKf + \frac{1}{n} Ln\ Ce$$

Where qmax (mg/g) is maximum adsorption capacity, qe (mg/g) is the adsorption capacity at equilibrium, b (mg/L) is the Langmuir constant, Ce (mg/l) is the equilibrium dye concentration in the solution, n represents the Freundlich constants and Kf is associated to the adsorption density.

2.6. Kinetics studies

The kinetics studies of the present adsorption process were performed to investigate the rate of the MB and CV adsorption by using the selected composite sheets which controls by an equilibrium time. The kinetics studies; pseudo first-order (1^{st}) and second-order (2^{nd}), were examined and the equations were expressed using the following equations **[27, 28].**

Pseudo-first-order equation:

$$Ln\ (qe - qt) = Ln\ qe - K1\ t$$

Pseudo-second-order equation:

$$\frac{t}{qt} = \frac{t}{K2qe^2} + \frac{t}{qe}$$

Where k_1 (min^{-1}) and K_2 (g/mg.min) are the pseudo first order and pseudo first order rate constant, respectively. qe and qt (mg/g) are the amount of adsorbed MB dye at equilibrium and at time t (min), respectively.

2.7. Desorption study

After implementation of the optimization process, the optimum factors were reinvestigated to confirm the result of the Response Optimizer and performing the reusing experiment. Ethanol concentrations 100 % were applied to explore the reusability of the selected composite sheets. Results were plotted and explained as 3Rs (Removal, Recover and Reuse) of the composite sheets for many times applications.

3. Results and discussion

3.1. Chemical composition of unhydrolyzed sugarcane bagasse wastes

The chemical composition (in terms of cellulose, hemicellulose and lignin) of sugarcane bagasse wastes before and after acid hydrolysis was investigated at various acid and biomass concentrations **[29]**. The materials were displayed as (1) 20g sugarcane bagasse waste treated with 2% H_2SO_4, (2) 20g sugarcane bagasse waste treated with 4% H_2SO_4, (3) 10g sugarcane bagasse waste treated with 4% H_2SO_4, and (4) 10g sugarcane bagasse waste treated with 2% H_2SO_4. In addition, sugarcane bagasse waste without any pre-treatment was used as a control. Results reported in **Table 1** showed that the control material has a higher cellulose and hemicellulose content of 41.29 and 37.02 %, respectively than lignin content of 21.69 %. While the concentrations of cellulose and hemicellulose in unhydrolyzed sugarcane bagasse wastes were dropped and the lignin content was increased after acid hydrolysis. The unhydrolyzed sugarcane bagasse waste (4) had a higher lignin content of 64.10% than the other unhydrolyzed sugarcane bagasse waste. This result was attributed to the high concentration of acid and the low concentration of sugarcane bagasse wastes during the acid hydrolysis process which cause a maximum degradation of hemicellulose followed by cellulose, resulting in an increase in lignin concentration.

Table (1): The chemical composition, cellulose, hemicellulose and lignin percent, of the sugarcane bagasse waste

Materials	Cellulose (%)	Hemicellulose (%)	Lignin (%)
Control	41.29	37.02	21.69
1	36.30	16.01	47.69
2	35.02	15.96	49.02
3	28.09	10.60	61.31
4	26.70	9.20	64.10

The Zeta potential of the unhydrolyzed sugarcane bagasse wastes was measured in order to detect the surface charges of them. The zeta potential data readings depended on the solution pH and had negative charges for all pH values (3.5, 4.5, 6.5, and 9.5) with the average zeta potential values of -16.3, -17.5, -9.13, -13.02, and -9.85 for the control, 1, 2, 3, and 4, respectively (see **Table 2**). The negative values of the zeta potential displayed the negativity of the material`s functional groups. This negativity groups were related to the hydroxyl and carboxylate groups in the materials. Therefore, this issue predicts an increase in cationic dyes removal.

Table 2. The zeta potential data of the sugarcane bagasse waste without any pre-treatment

Materials	pH values				Average
	3.5	**4.5**	**6.5**	**9.5**	
Control	-7.05	-14.8	-17.1	-26.5	-16.3
1	-4.59	-20.3	-20.6	-24.7	-17.5
2	-9.78	-13.5	-10.1	-3.16	-9.13
3	-11.2	-11.4	-11.4	-18.3	-13.0
4	-12.0	-9.09	-12.0	-6.33	-9.85

3.2. Characterization of the polymer sheets

3.2.1. Fourier transform infrared (FT-IR)

The FT-IR spectra of the blank sheet (cellulose acetate without any unhydrolyzed sugarcane bagasse wastes) and the control sheet (cellulose acetate with the sugarcane bagasse wastes without any pre-treatment) and the four composite sheets (1, 2, 3, and 4) performed from unhydrolyzed sugarcane bagasse wastes were displayed in **Figure (1)**. The results displayed well characteristic peaks of at 1741 cm^{-1} related to stretching of carbonyl (C = O) of acetate groups. The carboxylate C-O stretch appears around 1230 cm^{-1}, the peak at 1158 cm^{-1} corresponding to asymmetric stretching of C–O–C bridge, and the peak at 1043 cm^{-1}related to stretching of C–O–C pyranose ring. The peak for OH stretching vibration was appeared at 3472 cm^{-1}. The spectra of the composite sheets were the same spectra for the main polymer with slight shift in the position of peaks due to the similarity in the composition of the sugarcane bagasse waste and the cellulose acetate polymer.

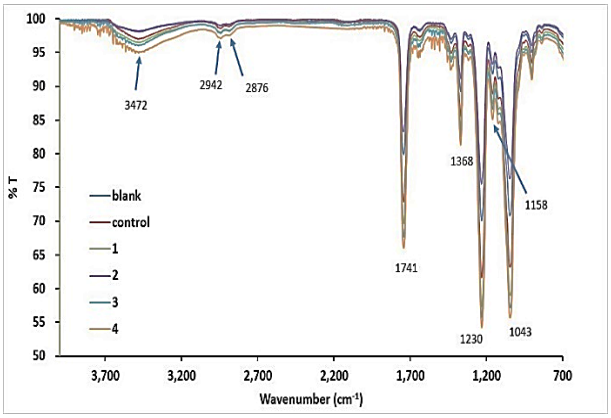

Figure 1. FT-IR spectra of the prepared composite sheets

3.2.2. X-ray diffraction (XRD)

The XRD pattern was used to determine the phase and the crystalline structure of the composite sheets, which can provide insights into their physical and chemical properties in addition to the blank and control sheets (see **Figure S1: a, b, c ,d, e** and **f**). The blank sheet showed a XRD pattern with peaks at 2θ = 21.4 and 25.1°. These peaks indicated the crystalline structure of the used cellulose acetate segments that obtained from aligned small chains of the main polymer. Furthermore, the XRD pattern of the composite sheets showed an additional peak around 9° which indicated the incorporation of cellulose moiety in the polymer matrix. The unhydrolyzed waste was expected to have high crystallinity that resist and prevent the acid hydrolysis through acid pre-treatment process. The (XRD) spectra of the composite sheets indicated the successful incorporation and compatibility of the sugarcane bagasse wastes and the polymer in one matrix.

3.2.3. Scanning electron microscopy (SEM)

The surface morphology of the blank sheet (cellulose acetate without any unhydrolyzed sugarcane bagasse wastes), the control sheet (cellulose acetate with the sugarcane bagasse substrate without any acid treatment), and the composite sheets (1, 2, 3, and 4) performed from unhydrolyzed bagasse wastes was examined using scanning electron microscopy (SEM) (see **Figure 2a, b, c**). The blank sheet surface was appeared as a smooth with no pores (**Figure 2a-left**). Whereas the composite sheets with unhydrolyzed sugarcane bagasse wastes displayed rough surfaces with more pores. Moreover, some particles (ground sugarcane bagasse wastes) on sheet the surface were also detected. The composite sheet with treated unhydrolyzed sugarcane bagasse waste (4) showed a higher pore density on the sheet surface, which may be due to the more hydrophilic nature of this sample that enhance pore formation during the phase inversion preparation process. It was clearly shown that, both the blank and the composite sheets have macro-voids cross- section structure (**Figure 2a, b, c ,-right**). The relatively low polymer content and the low viscosity of the casting solution may enhance the rate of solvent/nonsolvent exchange during the manufacturing processes that enhance macro-voids formation **[30]**. Moreover, the images displayed that the composite sheets had larger macro-void's structure than the blank sheet which can aid in the penetration of the dyes into the polymer matrix giving at the end a high adsorption capacity.

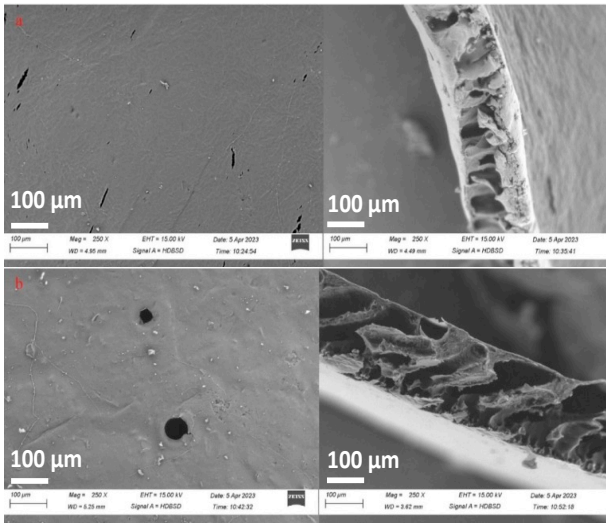

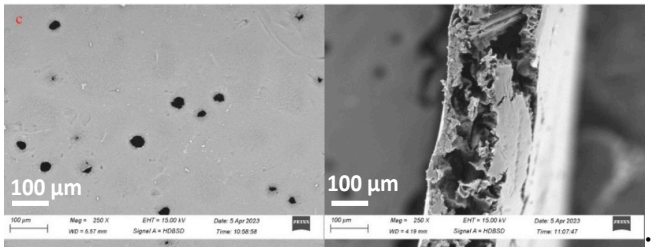

Figure 2: SEM of surface (left) and cross-section (right) of the blank sheet (polymer without any unhydrolyzed bagasse wastes) [a], the control sheet (polymer with the bagasse substrate without any acid treatment) [b] and one of the composite sheets (4) [c].

3.2.4. Swelling

The swelling behavior is usually used as an explanation of the hydrophilicity of the composite sheets. Results reported in **Table (3)** exhibited that the swelling behavior of the composite sheets was principally increased from 11.1% of the blank sheet to 66.7 % of the control sheet. The swelling was increased by incorporation of the unhydrolyzed sugarcane bagasse wastes to be in the range of 66.7 to 100 %. This result demonstrated that; the increase in the swelling behavior was attributed to the increase in extended hydrophilic functional groups of the composite sheets which composed mainly from unhydrolyzed sugarcane bagasse.

3.2.5. Porosity

The porosity values of the composite sheets were increased, like swelling behavior. The blank sheet porosity was 6.3 % in comparison to the control sheet with a porosity of 28.4 %. The porosity, as well, was increased by incorporation of the unhydrolyzed sugarcane bagasse wastes to achieved 28.8 % in the composite sheet (1). However, it decreased in the composite sheet 2 (18.1 %), 3 (21.12 %) and 4 (24.15 %) see **Table (3)**. The improvement of the porosity values can be attributed as well to the increase in extended hydrophilic functional groups of the composite sheets which composed mainly from unhydrolyzed sugarcane bagasse **[31]**. In addition, this improvement enhances the formation of the macro-voids. The results of the porosity were well agreed with the SEM cross section images. The improvement of the swelling and porosity characteristics predicted a good removal efficiency of dyes using the composite sheets.

Table 3: The swelling and the porosity measurements of the prepared sheets

Sheet`s type	Thickness (µm)	Swelling (%)	Porosity (%)
Blank	0.12	11.1	6.31
Control	0.12	66.7	28.49
1	0.16	66.7	28.85
2	0.13	66.7	18.10
3	0.23	87.5	21.12
4	0.26	100	24.15

3.3. Application of the composite sheets in the removal of Methylene Blue (MB) and Crystal Violet (CV) from contaminated wastewater

3.3.1. Screening experiment

Figure (3a, b) displayed the preliminary screening experiment that was implemented to determine the best pre-treatment methods that gives the highest Methylene Blue (MB) and Crystal Violet (CV) removal efficiencies in addition to the blank and control sheets. The results demonstrated that, the composite sheets 1, 3, and 4 displayed the highest removal efficiencies; 31.5, 30.6, and 26.5 % for the MB and 21.8, 15.9, and 28.1 % for the CV**.** Therefore, these sheets were selected for further optimization process.

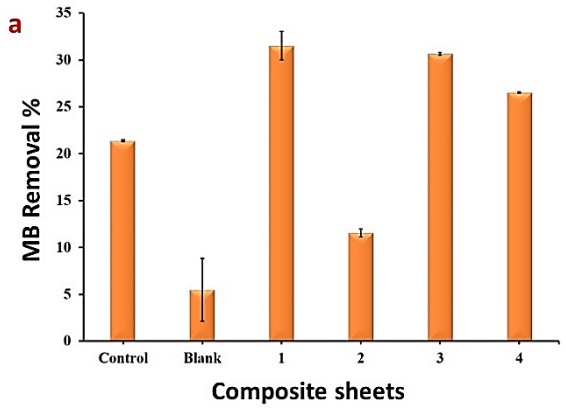

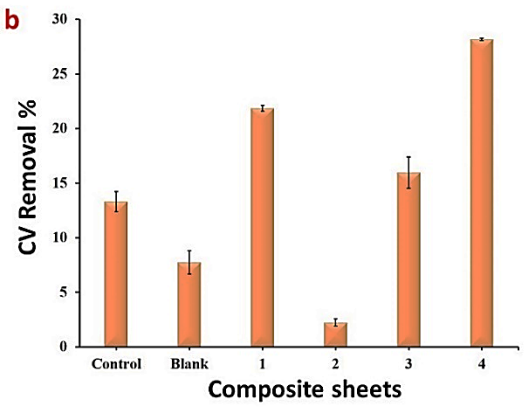

Figure 3: Screening experiment concerning the removal of (a) Methylene Blue (MB) and (b) Crystal Violet (CV) efficiencies using the selected composted sheets.

3.3.2. Optimization process

OFAT experiments

Effect of each factor on the Methylene Blue (MB) and the Crystal Violet (CV) removal efficiencies were studied according to OFAT. Optimum levels were applied to estimate the low and the high levels of the studied factors that latterly used in the factorial experiment (see **Table S1a, b)**.

Figure (4a, b) exhibited the effect of different contact time intervals on the MB and the CV adsorption by using the selected composite sheets (1, 3, and 4). The results demonstrated that the highest MB removal efficiencies of 29.9, 46.8, and 54.8 % were achieved after a contact time of 240 min using the selected composite sheets of 1, 3, and 4, respectively. Moreover, the highest CV removal efficiencies of 28.7, 26.0 and 34.2 % were accomplished after a contact time of 240 min using the selected composite sheets of 1, 3, and 4, respectively. The composite sheet 4 showed the highest removal efficiencies of the used dyes. It was noticed that, by increasing the contact time the removal efficiencies were increased. These could be related to the enormous active sites on the composite sheet`s surface, which are usually accessible in the initial state of the adsorption process, which in follow speedup the rate of adsorption in the initial time**.** Furthermore, by time, more dye`s particles were retained outside the composite sheet`s surface, hence the adsorption process became less favourable for the dyes removal **[32]**.

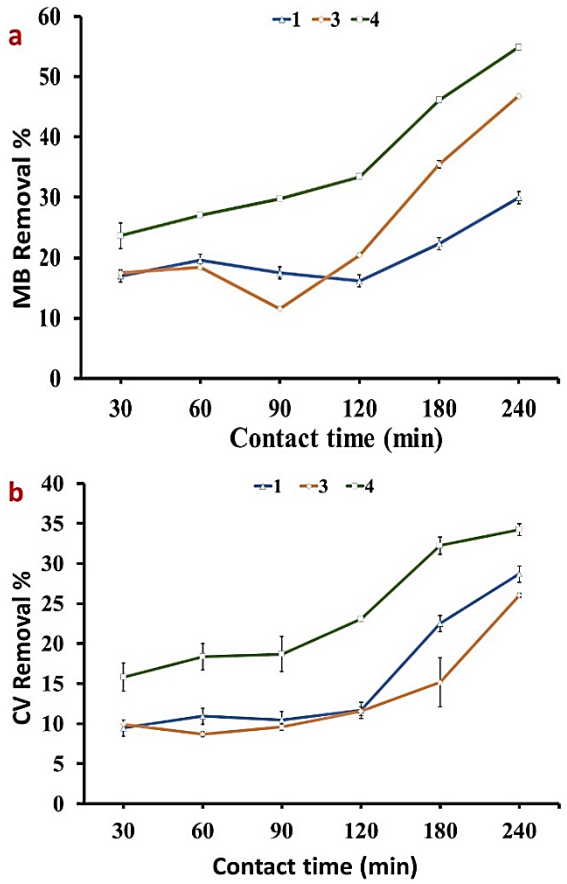

Figure 4: The effect of contact time intervals on (a) Methylene Blue (MB) and (b) Crystal Violet (CV) removal efficiencies using the selected composite sheets.

The effect of pH values on the adsorption process changed greatly by increasing or decreasing, as pH values change the ionization behaviour of the binding functional groups of both adsorbate and adsorbent. Therefore, it should be studied and optimized. The result was presented in **Figure (5a, b).** The MB, a cationic dye, removal efficiencies were increased by increasing the pH values. The highest MB removal efficiencies of 62.2, 65.7 and 70.3 % were achieved at a pH value of 6.5. Afterwards they decreased for the composite sheets 1, 3, 4, respectively. In the case of CV, a cationic dye, the highest removal efficiencies of 66.4, 65.9 and 65.8 % were obtained the same pH value (6.5) and after that they decreased. This result could be explained by increasing pH values, the OH^- ions increased the H^+ protons decreased that means increasing in the negative charges that further helps in the removal of the cationic dyes **[33]**.

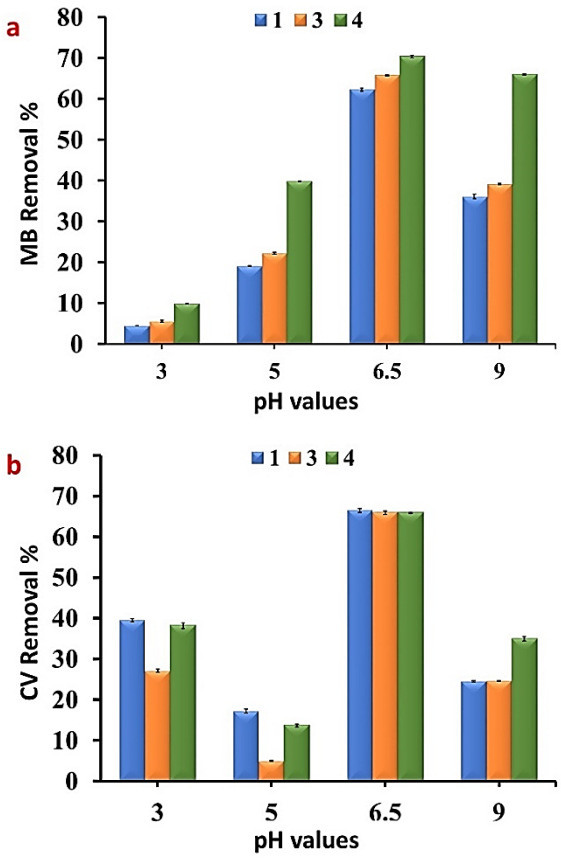

Figure 5: The effect of pH values on (a) Methylene Blue (MB) and (b) Crystal Violet (CV) removal efficiencies using the selected composite sheets.

It has been reported that, the increasing the adsorbent dose leads to an increase the surface area, including the active sites, hence achieve higher removal percent of the pollutant molecules **[34].** The increase in adsorption capacity by the increase in the adsorption dose was a reasonable result as a result of the availability of more reactive sites for removal process**.** However, this reasonable behavior can be displayed until a specific sorbent concentration after that a stability attitude for the adsorption process obtained as previously reported **[35].** The effect of the composite sheets dose on the MB and CV removal efficiencies were displayed in **Figure 6a, b,** respectively. For the cationic dyes MB and CV, the highest removal efficiencies were achieved at the composite sheets concentration of 3 g/l and afterwards a relatively the removal efficiencies slowly decreased

.

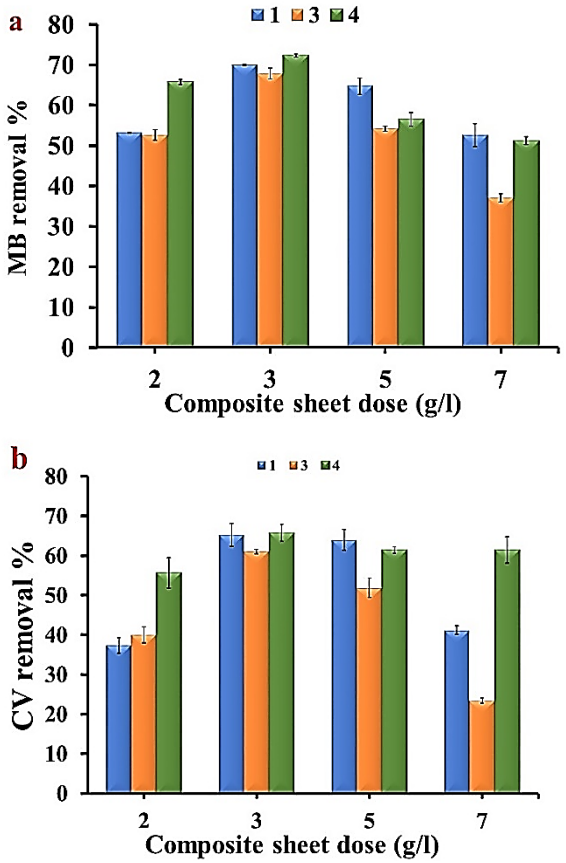

Figure 6: The effect of composite sheet dose on (a) Methylene Blue (MB) and (b) Crystal Violet (CV) removal efficiencies using the selected composite sheets.

Figure (7a, b) displayed the effect of the initial dye`s concentration on the removal efficiencies of the MB and CV dyes. The results showed that, a 100 ppm of the used dyes gave the highest removal efficiencies of by using the composite sheets. Moreover, by increasing the dye`s concentration, the removal efficiencies were decreased. Decreasing in the dyes removal efficiencies by rising the dye-concentration could be related to the early overload of the composite sheets by the number of dye ions until no further sites are available at the higher concentrations**[36].** The composite sheet 4 has displayed the highest removal efficiency for the used dyes (MB and CV).

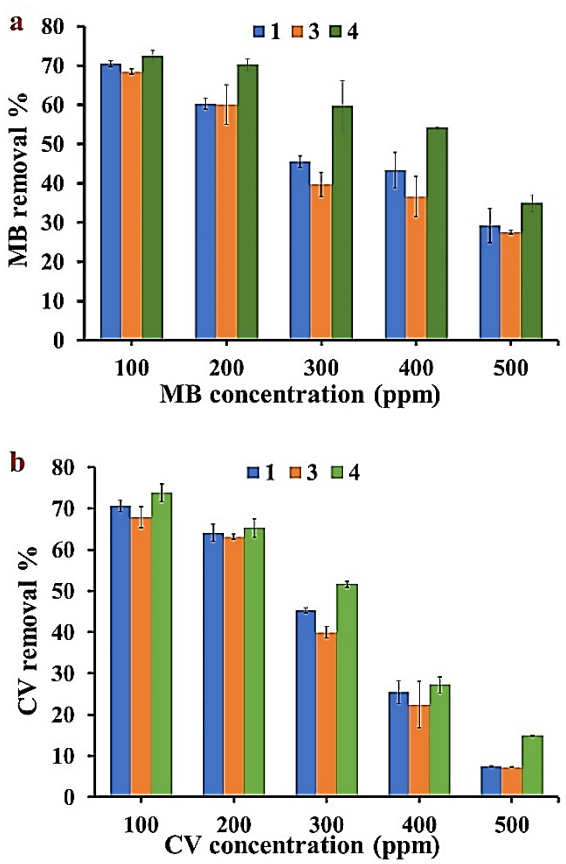

Figure 7: The effect of dye concentrations on (a) Methylene Blue (MB) and (b) Crystal Violet (CV) removal efficiencies using the selected composite sheets.

3.3.3. General Full Factorial Design

The matrix design including the removal efficiency fits and residuals were shown in **Table S2 (a, b).** Plots of main effects, interaction, Pareto and response optimizer were discussed as follows.

The main effects plots were displayed in **Figure S2 (a, b)** which determined the average deviation of each factor, from the low to high levels, where the removal efficiencies increased by increasing the deviation from the low to high levels **[37].** Whereas, they decreased by decreasing the deviation levels and considered as a negative effect on the removal percent. Results reported in in **Table S3-a**, and **Figure S2-a** demonstrated that, the deviation was increased from the low to high levels. Furthermore, the contact time, the composite sheet dose and the MB concentration have a compelling effect on the MB removal efficiency owning to the low P-value that was noticed in the ANOVA Table. All the factors displayed a positive effect on the MB removal efficiency where by increasing the values of the levels from the low to

high, the MB removal efficiencies were increased. Additionally, the results in **Table S3-b** and **Figure S2-b** exhibited that; the composite sheets dose and the CV concentration have a momentous effect on the CV removal efficiency and both of them affect positively.

Generally, the interaction effect is the studying of the interaction between the various factors to get the pollutant removal efficiently. When there is a change in a factor from low to high levels is dependent on a change in the factor's levels, such as when lines don't run parallel, accordingly, effective interaction is noticeable **[38]**. Results reported in **Table S4-a** and **Figure S3-a**, stated that, there is an interaction between the MB concentration & contact time and composite sheet dose &contact time. Furthermore, the three interactions effect of the MB concentration& composite sheet dose& contact time have a significant effect on the MB removal efficiency. Whereas CV removal efficiency exhibited none significant interacted factors as represented in **Table S4-b** and **Figure S3-b**.

The Pareto chart, in general, verified the main and interaction effects data. Student t-test result is represented in the Pareto chart by a reference line, and all the columns that exceed the reference line considers as significant values whereas, the columns that not exceed the reference lines is non-significant **[39].** The results outlined that, (AD) MB concentration& contact time, (D) contact time interaction effect, (ACD) MB concentration & composite sheet dose & contact ime, (A) MB concentration, (CD) composite sheet dose & contact time, and (C) composite sheet dose factors have a potent significant effect on the removal efficiency of MB (see **Figure S4-a**). Furthermore, **Figure S4-b** demonstrates that, (A) CV concentration, and (B) composite sheets type (treat) have the most significant effect on the CV removal efficiency. These results confirmed the obtained results from the main and interaction effects, which represented previously**.**

In fact, response optimizer predicts the optimum combined factors that achieve high pollutants removal efficiency as previously reported **[40]. Figure S5-a** demonstrated that; the highest removal efficiency of 90.36% was accomplished for MB with 1 degree of accuracy by using 5 g/l composite sheet dose of the treat sheet 4 for 100 ppm MB after 240 min contact time. **Figure (S5-b),** demonstrated that, the CV removal efficiency of 89.29 % could be achieved by using 7 g/l of the composite sheet 4 for removing 500 ppm CV after 240 min. by 1 degree of accuracy.

3.4. Langmuir and Freundlich isotherms

The isotherm studies were explored by the using two linear forms, Langmuir and Freundlich, to proposed the used dyes adsorption mechanism as seen in the **Figure 8 (a, b)** and **Figure 9 (a, b) [41].** The results of the MB and CV removal efficiencies, using the selected composite sheets (1, 3, and 4) performed from unhydrolyzed bagasse wastes, were more fitted with the Freundlich isotherm. This result in fact, was totally attributed to the higher "R^2" that determine the fitted model as previously reported **[42].**

Table 4a: The Langmuir and Freundlich isotherms of the Methylene Blue (MB) removal efficiency using the selected composite sheets (1, 3, and 4)

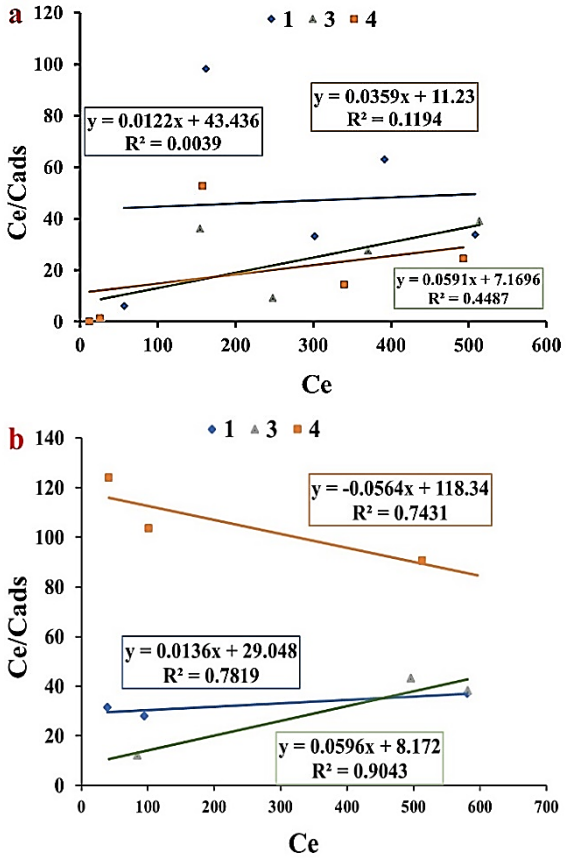

Figure 8: The Langmuir isotherm of (a) Methylene Blue (MB) and (b) Crystal Violet (CV) removal efficiencies using the selected composite sheets.

In general, fitting the data to the Freundlich isotherm displayed the mechanism of adsorption as a heterogeneous adsorption with a multilayer adsorption nature. Moreover, this adsorption nature was controlled by wander Val's forces. The maximum adsorption capacity (Q_{max}) of the selected composite sheets (1, 3, and 4) were represented in **Table 4 (a, b).**

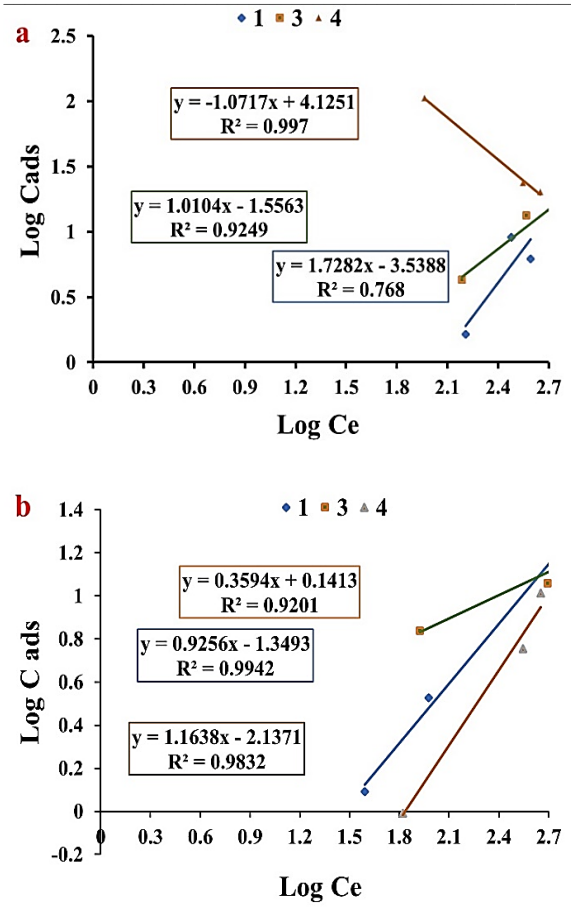

Figure 9: The Freundlich isotherm of (a) Methylene Blue (MB) and (b) Crystal Violet (CV) removal efficiencies using the selected composite sheets.

Table 4-a: The Langmuir and Freundlich isotherms of the Methylene Blue (MB) removal efficiency using the selected composite sheets (1, 3, and 4)

Langmuir isotherm			
	R^2	**b**	**Q_{max}**
1	0.0039	0.00028	81.97
3	0.448	0.00697	20.00
4	0.119	0.00267	33.33
Freundlich isotherm			
	R^2	**n**	**k**
1	0.77	0.58824	3457.80
3	0.92	0.98971	35.48
4	0.99	0.9331	13335.21

Table 4-b: The Langmuir and Freundlich isotherms of the Crystal Violet (CV) removal efficiency using the selected composite sheets (1, 3, and 4)

Langmuir isotherm			
	R^2	**b**	**Q_{max}**
1	0.78	0.00047	73.53
3	0.9	0.00745	16.78
4	0.74	0.00048	17.73
Freundlich isotherm			
	R^2	**n**	**k**
1	0.99	1.08108	22.34
3	0.92	2.78242	1.38
4	0.98	0.85985	137.12

3.5. Kinetics study

Result represented in **Figure S6 and S7** and **Table 5 (a, b)** exhibited the kinetics analysis plots in addition to their parameters. The correlation co-efficient "R^2" indicated that; the pseudo 2nd order was the fitted model of the MB and CV dyes removal using the selected composite sheets (1, 3, and 4). This result could be returned to the mentioned higher "R^2" of the pseudo 2nd order in addition to the result of the "q_e calculated" of the pseudo-order kinetic studies, which was near to the "qe experimental", unlike the state of the pseudo 1st order reaction **[43, 44].**

Table 5-a: The first (1st) and the second (2nd) order kinetics of the Methylene Blue (MB) removal efficiency using the selected composite sheets (1, 3, and 4)

1st order				
	R^2	**K**	**$Qe_{expr.}$**	**$Qe_{calc.}$**
1	0.39	0.00691	20.6	208.9
3	0.72	0.01474	32.34	2511.9
4	0.85	0.02027	37.9	3162.3
2nd order				
	R^2	**K**	**$Qe_{expr.}$**	**$Qe_{calc.}$**
1	0.9	0.000212	20.6	22.72727
3	0.89	0.000107	32.34	45.24887
4	0.85	9.99E-05	37.9	40.32258

Table 5-b: The first (1st) and the second (2nd) order kinetics of the Crystal Violet (CV) removal efficiency using the selected composite sheets (1, 3, and 4)

	1st order			
	R^2	K	$Qe_{expr.}$	$Qe_{calc.}$
1	0.57	0.01451	25.02	1406.0
3	0.22	0.01842	13.27	127.8
4	0.64	0.03777	29.9	4538.4
	2nd order			
	R^2	K	$Qe_{expr.}$	$Qe_{calc.}$
1	0.990	0.013719	25.02	7.87
3	0.770	0.001128	13.27	17.57
4	0.930	0.000391	29.9	35.5872

3.6. Reusability experiment

Figure 10 (a, b) demonstrated the reusability experiment where the highest efficient selected composite sheet (4) performed from unhydrolyzed bagasse wastes were applied successfully for five times in the process of 3Rs (Removal, Recover and Reuse) of the MB and the CV. Results obtained from the response optimizer were used to perform the reusability experiments. The results displayed the removal efficiencies of the MB and CV dyes were high at the first three runs then they declined in the fourth and fifth runs. The maximum removal efficiencies of around (95.6 and 97.3%) for the two dyes, respectively were achieved. The alcohol may dissociate the inter hydrogen bonding between the molecules of wastes and cellulose acetate which may increase the available reactive groups for adsorption resulted in enhanced the removal percentage. However after the third cycle the adsorbed dye molecules may be strongly tied to the adsorbate and need more condition as acid or base for desorb these molecules.

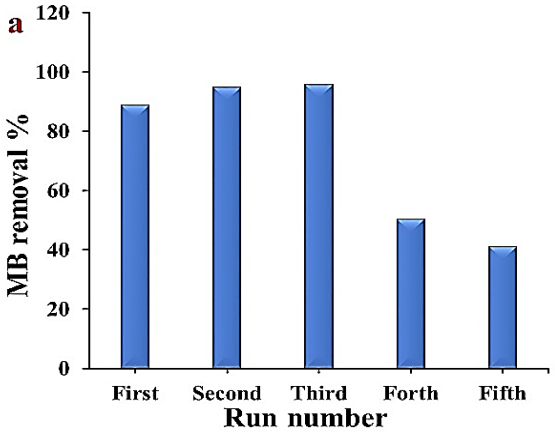

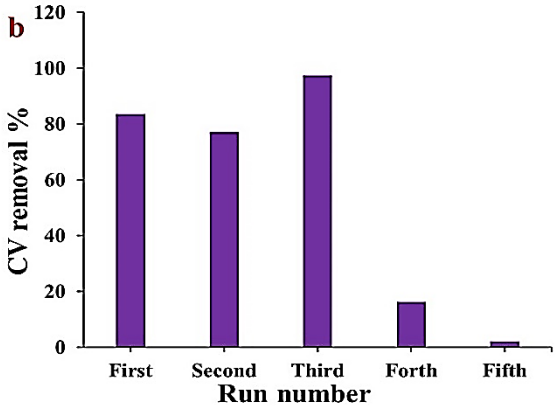

Figure 10: Reusability experiment of the highly efficient selected composite sheet (4) in the removal of (a) Methylene Blue (MB) and (b) Crystal Violet (CV).

4. Conclusion

Different residual wastes materials, after acids pre-treatment of collected sugarcane bagasse wastes that used in the production of bioethanol, (unhydrolyzed) were collected and ground using ball mill. The materials characteristics were interpreted by measuring the cellulose, hemicellulose and lignin percent in addition to assess their zeta potential values. The unhydrolyzed sugarcane bagasse wastes were successfully mixed with cellulose acetate polymer forming 5 composite sheets. The composite sheets were successfully interpreted by FT-IR, XRD and SEM in addition to swelling and porosity percent. The composite sheets were screened first for their highest removal of both Methylene Blue (MB) and the Crystal Violet (CV) removal efficiencies and the sheets, 1, 3, and 4 were chosen for further experiments. The composite sheets were optimized concerning the MB and CV removal efficiencies using OFAT followed by full factorial design experiments and the main & interaction effects, Pareto chart normal probability and the response optimizer were plotted and interpreted successfully. The highest removal efficiency of 90.36% was successfully attained for the MB with 1 degree of accuracy by using 5 g/l composite sheet dose of the treat sheet 4 for 100 ppm MB after 240 min contact time. While CV removal efficiency of 89.29 % was successfully achieved by using 7 g/l of the composite sheet 4 for removing 500 ppm CV after 240 min by 1 degree of accuracy. Freundlich isotherm and pseudo second order (2nd) kinetic were more fitted with the data obtained from the MB and CV removal

efficiencies. The reusability experiment results displayed the removal efficiencies of the MB and CV dyes were high (95.6 and 97.3%) respectively, at the first three runs then they declined in the fourth and fifth runs. For further investigation in the future, the composite sheets can be used through a reactor design in order to easy application of the removal process in the industrial and agriculture sectors.

Conflicts of interest

The authors confirm that there are no conflict of interest

Acknowledgments

The authors direct many thanks to National Research Center (NRC), and Egyptian Petroleum Research Institute (EPRI), Egypt for their providing and supporting by technical environment and tools.

References

[1] Abdelhafez, A., Metwally S. and Abbas H., Irrigation Water resources, types and common problems in Egypt. Technological and Modern Irrigation Environment in Egypt, Best Management Practices & Evaluation, 2020, **3** (6): p. 15-34.

[2] Allam, M. and Allam G.I., Water resources in Egypt: future challeges and opportunities, Water International, 2007, **32** (2-5):p. 205-218.

[3] Ashaal, T. and EL-Ramady H., Sustainable agriculture: towards holistic overview. Journal of Sustainable Agricultural Sciences, 2017, **43**(2):p. 65-67.

[4] Crini, G., Eric L., Lee W. and Nadia M.C., Conventional and non-conventional adsorbents for wastewater treatment, Environmental Chemistry Letters, 2017, **17**(15): p.195-213.

[5] Abdo M. H., Ahmed H. B., Helal M. H., Fekry M. M., Abdelhamid A. E., Water Quality Index and Environmental Assessment of Rosetta Branch Aquatic System, Nile River, Egypt, Egyptian Journal of Chemistry, 2022, **65** (4) p. 321-331

[6] El-Sadek, A. Virtual water trade as a solution for water scarcity in Egypt, Water Resources Management, 2010, **24** (11): p. 2437-2448.

[7] Rafatullah, M., Sulaiman O., Hashim R. and Ahmed A., Adsorption of Congo red on low-cost adsorbents: a review, Journal of hazardous materials, 2010, **177** (1-3): p. 70-80.

[8] Fatima M., Khalil A. M., Maurel F., Kadri A. and Chehimi M. M., Mixed oxide-polyaniline composite-coated woven cotton fabrics for the visible light catalyzed degradation of hazardous organic pollutants, Cellulose, 2020, **27,** 7823-7846.

[9] Abdelhamid A. E. and Kandil H., Facile approach to synthesis super-adsorptive hydrogel based on hyperbranched polymer for water remediation from methylene blue, Reactive and Functional Polymers, 2022, **177**, 105312

[10] El Jamal, M.M. and M.C. Ncibi, Biosorption of methylene blue by Chaetophora Elegans algae: kinetics, equilibrium and thermodynamic studies. Acta chimica slovenica, 2012. **59**(1): p. 24-31

[11] Hussein, S., Sulaiman O., Hashim R. and Ahmed A., Absorption of hexavalent chromium by green micro algae Chlorella sorokiniana: live planktonic cells, Water Practice and Technology, 2019, **14**(5): p. 27-33

[12] Elshabrawy, S.O., Elhussieny, A., Taha, M.M., Pal K., Fahim I.S., Wastewater treatment via sugarcane bagasse pulp. International Journal of Environmental Science and Technology, 2023, **20**, 12405–12416.

[13] Kamran, U., Bhatti H.N., Noreen S. and Tahir M.A., Chemically modified sugarcane bagasse-based biocomposites for efficient removal of acid red 1 dye: Kinetics, isotherms, thermodynamics, and desorption studies, Chemosphere, 2022, **291**(16): p. 132-796.

[14] Abo-State M. A., Ragab AME, EL-Gendy NS, Farahat L.A. and Madian H.R., Effect of different pretreatments on Egyptian sugarcane bagasse saccharification and bioethanol production, Egyptian Journal Petroleum, 2013, **22**:61–167.

[15] Saleh H. M. and Khalil A.M., Plastic Films Based on Waste Expanded Polystyrene Loaded with Bagasse Powder for Packaging Applications. Egyptian Journal of Chemistry, 2022, **65** (11) 323-329.

[16] .Moran-Aguilar M. G., Santoyo M. C., Oliveira R. P. S., Uscanga M. G. A and Domínguez J. M., Deconstructing sugarcane bagasse lignocellulose by acid-based deep eutectic solvents to enhance enzymatic digestibility, Carbohydrate Polymers, 2022, **1** (20): p. 5-10.

[17] Niju S. and Swathika M., Delignification of sugarcane bagasse using pretreatment strategies for bioethanol production, Biocatalysis and Agricultural Biotechnology, 2019, **20**: p.101-263.

[18] Abdelhamid A.E., Labena A., Mansor E.S., Husien Sh. and Moghazy R.M., Highly efficient adsorptive membrane for heavy metal removal based on *Ulva fasciata* biomass, Biomass Conversion and Biorefinery, 2023, **13**, 1691.

[19] Ahmed H.B., Helal M.H., Abdo M.H., Fekry M. M. and Abdelhamid A.E., Disarmament of micropollutants from wastewater using nylon waste/ chitosan blended with algal biomass as recoverable membrane, Polymer Testing, 2021, **104**, 107381.

[20] Gilbert, M. and Patrick S., Poly (vinyl chloride), in Brydson's Plastics Materials, 2017. Elsevier: p. 329-388.

[21] Jack C.I. and Leikin J. B., Methylene blue. American journal of therapeutics, 2003, **10**(4): p. 289-291.

[22] Labena A., Abdelhamid A.E., Husien S., Youssef T., Azab E., Gobouri A. A., and Safwat G., Grafting of Acrylic Membrane Prepared from Fibers Waste for Dyes Removal: Methylene Blue and Congo Red, Separations**,** 2021, **8**, 42.

[23] Rabiee, H., Vatanpout V. and Zarrabi H., Improvement in flux and antifouling properties of PVC ultrafiltration membranes by incorporation of zinc oxide (ZnO) nanoparticles. Separation and purification technology, 2015, **156**: p. 299-310.

[24] Kamran, U., Chemically modified sugarcane bagasse-based biocomposites for efficient removal of acid red 1 dye: Kinetics, isotherms, thermodynamics, and desorption studies. Chemosphere, 2022, **29** (1): p. 132-796.

[25] Langmuir, I. The adsorption of gases on plane surfaces glass, mica and platinum. Journal of American Chemical Society, 1918, **40(9)**: p. 1361–1403.

[26] Freundlich, H., Über die adsorption in lösungen Zeitschrift für Physikalische Chemie, 1970, **57** (12): p 385–470.

[27] Nandi, B.K., Goswami A., and Purkait M.K., Removal of cationic dyes from aqueous solutions by kaolin: Kinetic and equilibrium studies. Applied Clay Science, 2009, **42** (3): p. 583-590.

[28] Aksakal, O. and Ucun H., Equilibrium, kinetic and thermodynamic studies of the biosorption of textile dye (Reactive Red 195) onto Pinus sylvestris L. Journal of Hazardous Materials, 2010, **181** (1): p. 666-672.

[29] Sluiter, A., Hames B., Ruiz R., Scarlata C., Sluiter J., Templeton D. and Crocker D., Determination of structural carbohydrates and lignin in biomass. Laboratory Analytical Procedure, 2008, **16** (7) :P. 1–16.

[30] Orabi A.H., Abdelhamid A.E., Salem H.M. and Ismaiel D.A., Uranium removal using composite membranes incorporated with chitosan grafted phenylenediamine from liquid waste solution, Cellulose, 2021, **28,** 3703-3721

[31] Selim S. E., Meligi G. A. , Abdelhamid A.E., Mabrouk M. A. and Hussain A. I., Novel Composite Films Based on Acrylic Fibers Waste/Nano-chitosan for Congo Red Adsorption, Journal of Polymers and the Environment, 2022, **30**, 2642–2657

[32] Alver, E. and Metin A.Ü.. Anionic dye removal from aqueous solutions using modified zeolite: Adsorption kinetics and isotherm studies. Chemical Engineering Journal, 2012, **200** (6): p. 59-67.

[33] Beltrán T., Heredia J. and Sánchez Martín J.. Azo dye removal by Moringa oleifera seed extract coagulation. Coloration Technology, 2008, **124**(5): p. 310-317.

[34] Hang, C. and Hang J., Study of the desorption of hydrolysed reactive dyes from cotton fabrics in an ethanol–water solvent system, Coloration Technology, 2014, **130**(2): p.81 85.

[35] Travlou, N.A., Graphite oxide/chitosan composite for reactive dye removal. Chemical Engineering Journal, 2013, **217(20)**: p. 256-265.

[36] Ponnusami, V., Biosorption of reactive dye using acid-treated rice husk: factorial design analysis. Journal of hazardous materials, 2007, **142**(1-2): p. 397-403.

[37] Kazemi, J. and Javanbakht V., Alginate beads impregnated with magnetic Chitosan@ Zeolite nanocomposite for cationic methylene blue dye removal from aqueous solution. International journal of biological macromolecules, 2020, **154**: p. 1426-1437.

[38] Nandi, B.K., Goswami A., and Purkait M.K., Removal of cationic dyes from aqueous solutions by kaolin: Kinetic and equilibrium studies. Applied Clay Science, 2009, **42**(3): p. 583-590.

[39] Tran, T.H., Adsorption isotherms and kinetic modeling of methylene blue dye onto a carbonaceous hydrochar adsorbent derived from coffee husk waste, Science of the Total Environment, 2020, **725**: p. 138-325.

[40] Bingol, D., Tekin N., and Alkan M., Brilliant Yellow dye adsorption onto sepiolite using a full factorial design. Applied clay science, 2010, **50**(3): p. 315-321.

[41] Tang M., Snoussi Y., Bhakta A. K., El Garah M., Khalil A.M., Ammar S. M., and Chehimi M. M, Unusual, hierarchically structured composite of sugarcane pulp bagasse biochar loaded with Cu/Ni bimetallic nanoparticles for dye removal. Environmental Research, 2023, **232**, 116232.

[42] Pigorsch E., Spectroscopic Study of pH and Solvent Effects on the Structure of Congo Red and its Binding to Amyloid-Like Proteins, Fifth International Conference on the Spectroscopy of Biological Molecules. 1993. Springer.

[43] Penchev H., Abdelhamid A. E., Ali, E. A. Budurova D., Grancharov G., Ublekov F., Koseva N., Zaharieva K., El-Sayed A. A., and Khalil A. M., Novel Electrospun Composite Membranes Based on Polyhydroxy butyrate and Poly (vinyl format) Loaded with Protonated Montmorillonite for Organic Dye Removal: Kinetic and Isotherm Studies, Membranes, 2023, **13**(6) 582.

[44] Salah H., Abdelhamid A. E., Moghazy R.M. and Amin A., Functionalized PVA film with good adsorption capacity for anionic dye, Polymer Engineering and Science, 2022**, 62**, 145